Solid State Phenomena
ISSN: 1662-9779, Vol. 390, pp 11-18
doi:10.4028/p-4ggPVB

Submitted: 2025-12-17
Revised: 2026-02-16
Accepted: 2026-02-21
Online: 2026-04-17

A Novel Approach for Determining the Bauschinger Effect in Dual-Phase Steel Sheets with Tensile-Compression Tests

Adam Häckel[1,a*], David Naumann[1,b], Marion Merklein[1,c]

[1]Institute of Manufacturing Technology, Friedrich-Alexander-Universität Egerlandstraße 13, 91058 Erlangen, Germany

[a*]adam.haeckel@fau.de, [b]david.naumann@fau.de, [c]marion.merklein@fau.de

*corresponding author

Keywords: material characterization, dual-phase steels, bauschinger effect.

Abstract. In order to reliably predict a material's behavior during the forming process, robust calculations with precisely calibrated material models are required. Especially when it comes to mapping phenomena depending on complex interactions of different effects, sophisticated measuring techniques have to be used in order to capture them sufficiently. Springback of sheet metal components is governed by elastic behavior, determined by geometry and current material properties. While well understood for most materials, dual-phase steels are exceptional due to their non-linear elasticity and pronounced kinematic hardening, which strongly affect elastic response. Kinematic hardening is characterized via the Bauschinger coefficient from tension–compression tests. As the Bauschinger effect depends on pre-strain and strain rate, precise crosshead control is essential. Therefore, state-of-the art characterization techniques control the process speed by calculating the crosshead velocity from the pre-set clamping length and strain rate. This method, however, does not account for setup-related influences such as machine stiffness or specimen slippage. Therefore, to improve the characterization accuracy of the Bauschinger effect, an alternative method for crosshead control during the tensile-compression test is introduced and analyzed in this study. To compare this innovative approach with the conventional one, both methods are used to capture the effect of relaxation on the Bauschinger effect with different dual-phase and mild steel. The mentioned novel method is based on the optical strain rate control during tensile tests by Naumann, using Digital Image Correlation with an Aramis setup by ZEISS. The intended pre-strain before load reversal is actively controlled by measuring the strain in situ. After characterizing the material cards for each setup, the resulting Chaboche-Rousselier curves are compared to the experimental ones. The results demonstrate that the applied method provides a reliable proof of concept and achieves precision comparable to, as well as exceeding, the conventional displacement strain rate control method.

Introduction

Dual-phase steels (DP steels) were developed in the 1970s based on low-carbon microalloyed sheet steels for the automobile industry. Due to their excellent balance of strength, ductility and energy absorption, they are one of the most widely produced advanced high strength steels (AHSS), leading to their standardization in the 2000s. To date, however, the elastic-plastic material behavior of DP steel is not fully understood, which manifests as inaccuracies during numerical predictions, especially during springback prognosis simulations. The main difficulty hereby lies in describing the complex interactions between several material and forming process related effects, ranging from the micro- to the macroscale. These effects are predominantly the Bauschinger effect [1], non-linear elasticity [2], pre-strain [3] as well as strain rate [4]. Various sophisticated material models have been developed in the last decades tackling this challenge and providing the tools for highly accurate numerical simulations. Specially for predicting the springback of DP steels after sheet forming processes, the hardening models developed by Chaboche and Rousselier (CR) [5] as well as Yoshida and Uemori [6] are widely adopted. Calibrating these models however, requires extensive material characterization of high precision, such as tensile-compression tests (TCT), compression-tensile tests (CTT) along with regular tensile and compression tests. While associated challenges, such as buckling

during compression [7] or precise strain measurements despite localized necking [8] have been addressed thoroughly, strain rate dependency remains an issue, especially for springback related predictions of DP-steels.

The Bauschinger effect describes the phenomenon whereby a metal that has been plastically deformed in one direction exhibits a reduced yield stress when the loading direction is reversed, compared to the forward direction [9]. At its core, the effect arises from the internal stress state created during forward plastic deformation. Dislocations accumulate and interact with obstacles such as grain boundaries, precipitates or phase interfaces, leading to heterogeneous microstructures with regions of high and low dislocation density [10]. These heterogeneous dislocation structures give rise to back-stresses, which are categorized as long-range internal stresses that oppose further forward deformation but assist the onset of plasticity upon load reversal. Under reversed stress, dislocations encounter reduced resistance and can remobilize at lower applied stress, resulting in the lowered reverse yield strength characteristic of the Bauschinger effect [11]. The magnitude of the effect depends on microstructural factors such as grain size, dislocation density, phase distribution, and precipitate content, as well as on loading conditions including pre-strain level, strain rate, and temperature. In alloys and steels with multiple phases, differences in plastic incompatibility between phases enhance residual stress gradients and thus accentuate the Bauschinger effect [10]. During cyclic deformation, the transient component of the effect leads to an initial rapid reduction in yield stress upon load reversal, followed by a more stabilized response as the reversed deformation progresses. Thermally activated processes, such as dislocation climb or recovery, can mitigate back-stresses if hold times or temperatures are sufficient, thereby modifying the Bauschinger response. The Bauschinger effect is most commonly described using equation (1) [9], determining the Bauschinger coefficient (BC) as the absolute ratio between the stress before load reversal (σ_1) and re-yielding after (σ_2).

$$BC = \left|\frac{\sigma_2}{\sigma_1}\right|. \tag{1}$$

To investigate relaxation effects on elastic-plastic material behavior with industrial relevance, relaxation mechanisms on a timescale of seconds must be considered. The dominating effects in the first seconds during relaxation are rearrangements and gliding of dislocations, cross-slip as well as microplastic redistribution between phases, such as ferrite and martensite [12]. These effects however, can already be activated during forming, depending on the applied strain rate [10]. Therefore, the influence of a strain controlled holding time may be diminished due to slow strain rates [13].

If conventional tensile tests are carried out by applying displacement strain rate control (DSRC), strain and strain rate are calculated by the crosshead position during testing. This negatively affects the accuracy of the strain rate through influences like machine compliance and specimen clamping. With the conventional DSRC setup, a compensation of machine influences is necessary. Because of the specimen's slippage between the clamps, the initial clamping length cannot be taken into account accurately when it comes to reaching the intended pre-strain before load reversal. To compensate the discrepancy between the intended and the actually achieved strain, a preliminary investigation with separate tensile and compression tests is conducted. By measuring the achieved true strain with a digital correlation system (DIC), the traveled distance of the crossbeam can be matched with the corresponding true strain. This workaround is required for every testing configuration (material, pre-strain, strain rate, etc.) and poses an inefficient use of resources. To overcome this challenge, different approaches have been presented in the past and also were converted into standards like the ISO 6892-1 method A1. Thereby, a closed loop control is applied with a strain measurement system, which directly determines the strain at the gauge length of the specimen. Tactile and optical measuring systems can be used for this purpose. Further development was done by Naumann and Merklein by utilizing local optical strain rate control (OSRC) with DIC to account for local strain phenomena like diffuse and localized necking [14]. This not only makes it possible to specifically influence and thus control the strain rate on the sample, but also the strain itself. As an attempt to enhance the experimental characterization of the Bauschinger effect and consequently improving the calibration

of state-of-the-art hardening models such as the Chaboche-Rousselier and Yoshida-Uemori models, this paper introduces a method of conducting strain and strain rate controlled tensile-compression tests utilizing a DIC setup.

Setup and Methodology

All tests were carried out on universal testing machines from ZwickRoell with a nominal force of 100 kN and a maximum crosshead speed of 600 mm/min and 1500 mm/min. A special tool design along with the miniaturized specimen geometry is presented by Staud and Merklein [7]. They were used to apply defined tension and compressive loads to the specimens. The specimens with an initial gauge length and width of 2 mm were laser cut and subsequently wire cut by electrical discharge machining in the area of free span between the clamping jaws to reduce the influence of edge quality. Clamping was done by hydraulic pressure and force closure. The individual components are displayed in Fig. 1. The relatively short gauge length enables compression strains to a certain level without the risk of buckling and also without friction influence as it would appear with an anti-buckling device.

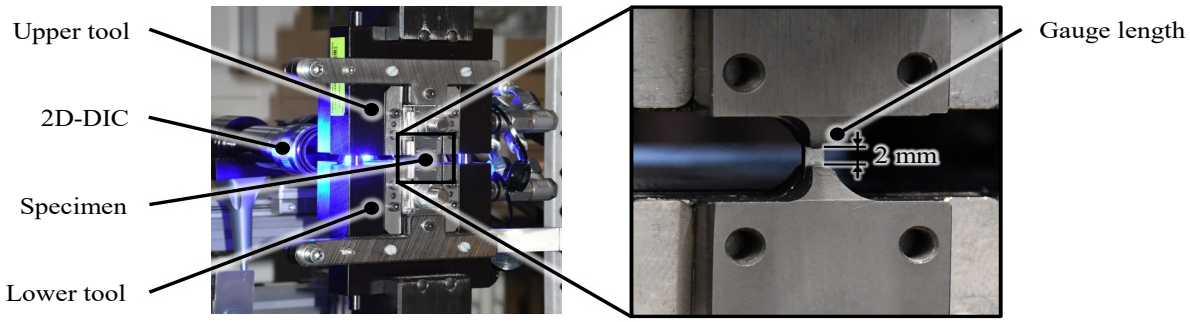

Fig. 1. Test setup for the tensile-compression-tests with 2D-DIC.

The strains were measured contactless by a two-dimensional digital image correlation system from Zeiss ARAMIS with a 12 Mpx camera setup. The closed control loop was built up between the electronic control unit (ECU) of the universal testing machine (UTM) and the ARAMIS DIC-system. Strains were live calculated over a gauge length of 1 mm by a virtual extensometer on the specimen surface and fed back to the ECU with a 0 to 10 V analog signal. The control of the crosshead movement was calculated by an embedded PID-controller of the ECU. Post processing of the strains was done by an analyzed area of 1.5 x 1.5 mm², where strains were averaged to reduce measurement noise and measurement errors. Three different steel grades with a nominal thickness of 1 mm were investigated in the scope of this contribution. Table 1 shows the different configurations of the investigation, varying material, type of strain rate control, relaxation holding time and pre-strain.

Table 1. Varied parameters for tensile-compression tests.

Material	Strain rate control	Holding time [s]	Strain [%]
DC04	DSRC	0	1
DP600			1.5
DP1000	OSRC	10	2
			3
			5

A mild steel DC04, and two AHSS with a dual-phase composition of martensitic phase embedded in a ferritic matrix DP600 and DP1000 are used in the TCTs in rolling direction. A constant strain rate of $\dot{\varepsilon} = 0.1$ %/s is intended to achieve, providing a control loop designed to be as robust as possible. As a final step, the experimental stress-strain-curves of the TCT are used to characterize the kinematic hardening behavior and to calibrate the Chaboche-Rousselier constitutive model. The material response is described using a nonlinear kinematic hardening formulation, in which the total back stress is defined as the superposition of individual back-stress components α_i, represented by equation

(2). Considering the uniaxial nature of the TCT, the Armstrong-Frederick evolution equation, used by the CR constitutive equations, simplifies to equation (3) [5]. $\dot{\varepsilon}^p$ is the plastic strain rate tensor. C_i and γ_i are the material parameters. As literature suggests, two CR-terms (N = 2) are used [15]. The material parameters are identified with the non-linear least-square Fit method (Isqnonlin) by fitting the tensile and compression segments of the stress-strain curve, minimizing the error in stress between data and model [16].The final difference between the experimental and modelled stress-strain curve is presented as the root mean square error (RMSE).

$$\alpha = \sum_{i=1}^{N} \alpha_i. \quad (2)$$

$$\dot{\alpha}_i = C_i \dot{\varepsilon}^p - \gamma_i \alpha_i |\dot{\varepsilon}^p|. \quad (3)$$

Results

In the following, the results of the TCTs are presented. The stress-strain curves as well as the strain rate over the true strain with the target strain of $\varepsilon = 0.05$ and nominal strain rate of $\dot{\varepsilon} = 0.1$ %/s are used to compare the OSRC with the DSRC method. The influence of relaxation with a holding time of 10 s (t10) compared to 0 s (t0) for the materials DC04, DP600 and DP1000 is investigated. Additionally, the averaged Bauschinger coefficients (BC) are plotted against the achieved true strain for every test configuration. In Fig. 2, the reference measurements with DC04 are shown. While an influence of relaxation is not discernible between t0 and t10 for both control methods, the stress-strain curves, however, show a distinct difference in the measured true strain between DSRC and OSRC.

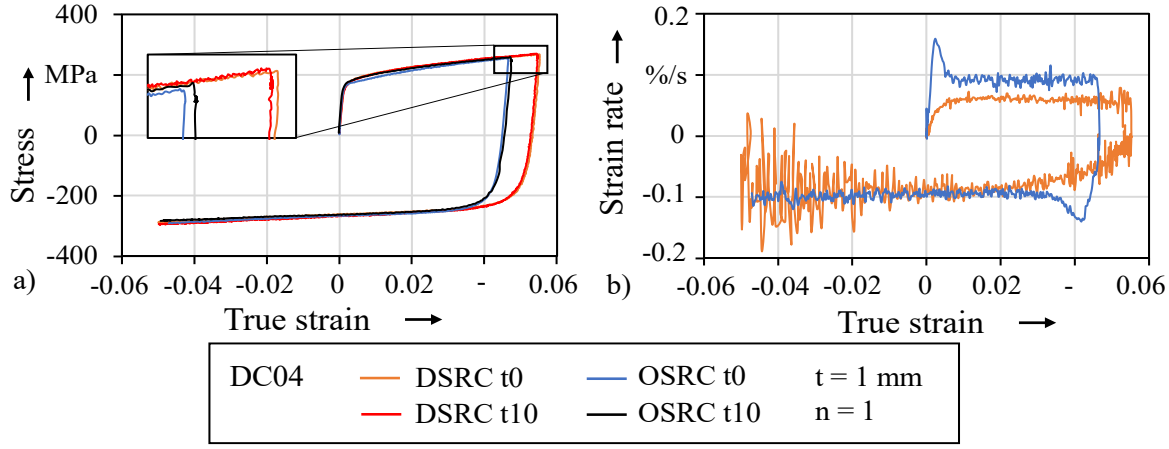

Fig. 2. a) Stress-strain curve and b) strain rate over true strain for DC04.

While the strains for OSRC deviate from the target strain with $\varepsilon = 0.047$, the DSRC method overshoots with $\varepsilon = 0.054$. The actually measured strain rate of the observed area highlights the success of the OSRC method in regulating the strain rate. After an initial overshoot, the strain rate stabilizes at 0.092 ± 0.006 %/s during the tensile segment and at -0.097 ± 0.006 %/s during compression. DSRC also provides a near constant strain rate for DC04 with an average tensile strain rate of 0.059 ± 0.007 %/s and an irregularly erratic compression strain rate. The deviating strain rates of DSRC show the distinct difference between the strain rate control methods. As DSRC provides a constant tensile strain rate, it misses the targeted rate due to the imprecisely set clamping length. After load reversal, the DSRC strain rate closes in on the target rate. It diverts, however into a highly irregular strain rate inside the measured area. OSRC on the other hand provides flexible adjustment of the crossbeam, controlled by the in-situ measured true strain, a highly reliable strain rate across the whole testing cycle.

Fig. 3 shows the typical stress-strain curves for DP600 with less pronounced elastic-plastic transitions after load reversal. The total tensile and compression strains behave similarly to the DC04 specimens with DSRC overshooting ($\varepsilon = 0.052$) and OSRC undershooting ($\varepsilon = 0.048$) the target value. For DP600 no influence of relaxation is noticeable in the stress-strain curves. The DSRC strain rate curve

of the observed area is severely erratic, while OSRC provides a steady tensile strain rate of 0.095 ± 0.005 %/s and a compression strain rate of -0.097 ± 0.007 %/s. In Fig. 4, the total true strains of DP1000, in contrast to DC04 and DP600, overlap for DSRC and OSRC mostly, with OSRC being closer to the target strain with 0.048 than DSRC with 0.047.

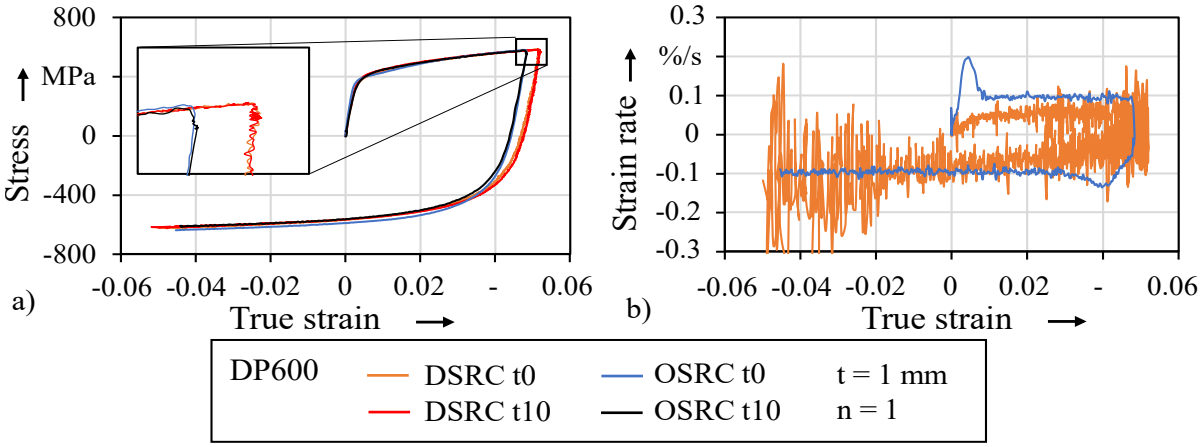

Fig. 3. a) Stress-strain curve and b) strain rate over true strain for DP600.

Apart from the longer overshoot observed in Fig. 4b) which results from the higher strength and consequently larger elastic strain of DP1000 compared to DC04 and DP600, the strain rate of the OSRC setup proves to be reliably consistent for all three materials. The tensile strain rate of DP1000 was 0.095 ± 0.006 %/s, without prior mapping of each configuration's elastic-plastic behavior. The DSRC strain rates, however, do not reach the intended strain rate for all configurations and also differ for each material. This highlights the DSRC's dependency on the material's strength and therefore the need of subsequent, often iteratively conducted pre-examinations for each particular setup. The absence of an influence due to relaxation in the stress-strain curve is attributed to the small strain rate of 0.1 %/s used in the TCTs, activating most relaxation mechanisms during plastification.

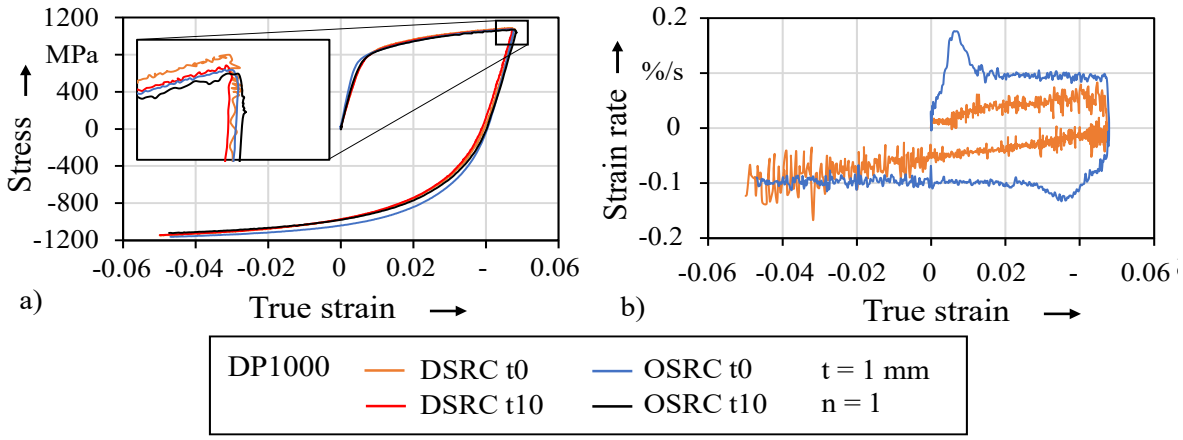

Fig. 4. a) Stress-strain curve and b) strain rate over true strain for DP1000.

The determined and averaged Bauschinger coefficients for the steels DC04, DP600 and DP1000 across engineering pre-strains of 1 %, 1.5 %, 2 %, 3 % and 5 % are presented in Fig. 5. The resulting plastic strains differ between materials because the target values were defined in terms of engineering strain, not considering elastic strain. Consequently, materials with higher elastic fractions reached lower plastic strains at the same nominal pre-strain. The measured evolution of BC follows a trend that can be approximated by a power-law relationship. Nevertheless, some data points slightly deviate from this behavior and fall outside the corresponding fit. The overall small standard deviation of the Bauschinger coefficient demonstrates the repeatability of the conducted experiments, especially for the OSRC method.

The comparison between DSRC and OSRC reveals that the Bauschinger coefficients are slightly but consistently higher under OSRC than under DSRC. This difference could be attributed to the constant strain rate loading at 0.1 %/s under OSRC, in contrast to the first lower but accelerating strain rate with higher fluctuations under DSRC. The constant strain rate enables a first relaxation of the initially induced back stresses by the overshoot during elastic strain, while an accelerating strain rate causes back-stresses to build up instead, resulting in a stronger Bauschinger effect. In addition, transient effects immediately following load reversal may contribute to a rapid, short-lived drop in yield stress, which decays within a small strain interval. Under OSRC, these transient contributions, together with the pre-relaxed back-stress field, may slightly modify the early reversal response, whereas under DSRC they appear less pronounced. Relaxation holds have little influence on the coefficient for DSRC, while for OSRC a slight reduction in BC is observed, following the hold. This behavior could be interpreted as the hold activating the remaining relaxation potential after the relaxation inducing slow loading process. The exact mechanisms responsible for these subtle trends are not yet fully clarified, and further targeted experiments would be required to achieve a comprehensive understanding.

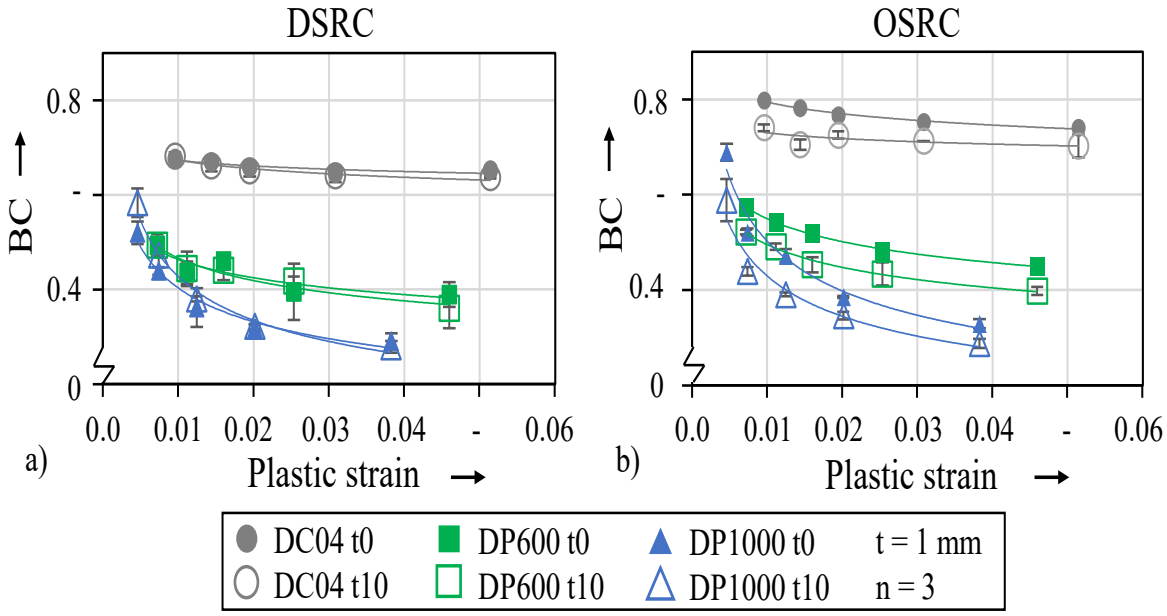

Fig. 5. Bauschinger coefficients over plastic strain with approximated trendlines following a power law for a) DSRC tests and b) OSRC tests.

The Chaboche-Rousselier parameters were identified by fitting the model response to the experimentally measured stress-strain curves of the TCT, focusing on the accurate reproduction of the transition from forward plastic deformation to re-yielding in compression. The fitting procedure minimized the deviation between experimental and model curves over the relevant strain range, with emphasis on capturing the curvature and saturation behavior of the kinematic hardening response. As presented in Fig. 6, the fitted CR-model curves yield consistent results. The OSRC curves achieve equally low RMSE compared to the DSRC results, rising respectively for higher strength materials. This degree of deviation from the experimental stress-strain-curves aligns with previous investigations on the Chaboche-Rousselier hardening model [17], validating the suitability of the OSRC method for material card calibration.

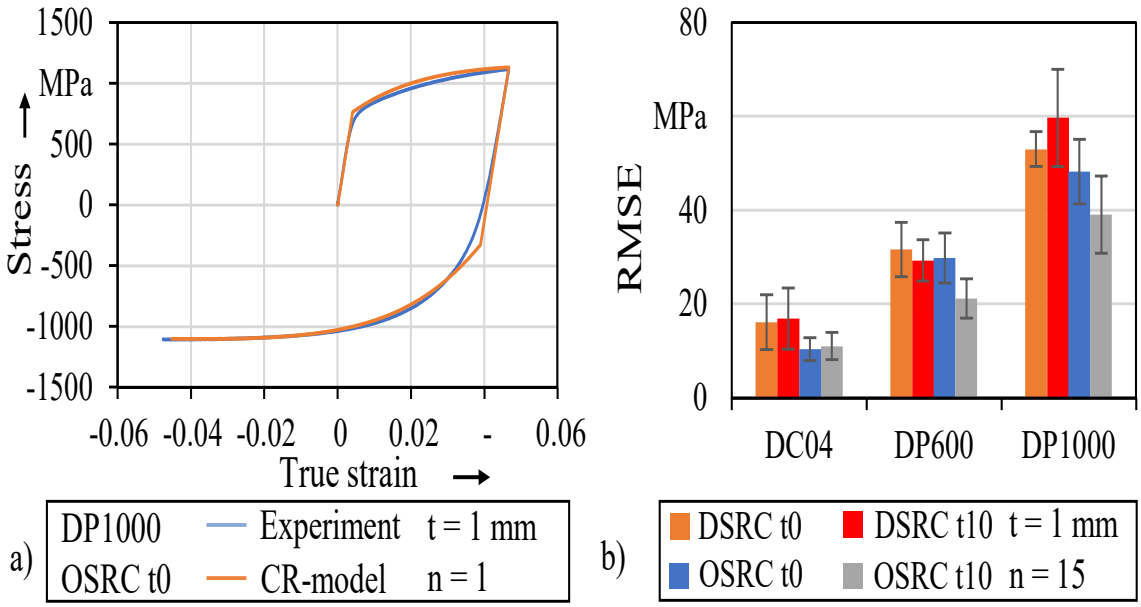

Fig. 6. Comparison of fitted curve deviation a) single curve of DP1000 OSRC t0 b) mean value and standard deviation of all specimens RMSE values compared by configuration.

Summary and Outlook

The study reaffirms the proof of concept for the optical strain rate control methodology by Naumann and Merklein [14] by demonstrating its applicability to reverse loading experiments, a domain in which reliable local strain rate control has so far remained insufficiently addressed. By overcoming limitations of conventional displacement-based control strategies, the presented results highlight the potential of optical strain rate control to close an important methodological gap in the experimental characterization of cyclic and reverse plasticity. The results show that OSRC attains a level of measurement precision comparable to, and in some cases exceeding, that of displacement-controlled approaches. Mean deviations of the Bauschinger coefficient remain similarly low, and the RMSE values of the fitted Chaboche-Rousselier curves are consistently as low as those obtained with DSRC. Moreover, the RMSE of the CR-parameter identification demonstrates that OSRC is fully suitable for material parameter calibration, providing a level of fidelity that aligns with established standards. A central advantage of OSRC is the increased control over the experimental setup. The strain as well as the strain rate can be regulated directly within the optically tracked region of interest. It ensures a more accurate representation of the local deformation. In addition, the method requires no mechanical workarounds and can be rapidly implemented within existing optical measurement infrastructures.

Future work should investigate how OSRC affects the stability and accuracy of calibrated material parameters, particularly in numerical and experimental sheet-metal forming applications. Further development of the software environment could enhance usability and streamline data processing. Extending the methodology to higher strain rates and elevated temperatures will help assess its robustness under more demanding conditions.

Acknowledgement

The authors would like to thank the German Research Foundation (DFG) for funding the project “Analysis of the elastic-plastic material behavior of higher strength steel materials under cyclical and swelling load in dependence of the relaxation behavior” (Project number 519030020).

References

[1] K. Yilamu, R. Hino, H. Hamasaki, and F. Yoshida, "Bauschinger Effect on Springback of Clad Sheet Metals in Draw Bending," Mater. Trans., vol. 51, no. 7, S. 1364–1366, 2010.

[2] L. Wagner, M. Wallner, P. Larour, K. Steineder, and R. Schneider, "Reduction of Young's modulus for a wide range of steel sheet materials and its effect during springback simulation," IOP Conf. Ser.: Mater. Sci. Eng., vol. 1157, no. 1, p. 12031, 2021.

[3] K. Barienti, M. Klein, S. Wackenrohr, S. Herbst, F. Nürnberger, and H. J. Maier, "Influence of Pre-strain on Very-Low-Cycle Stress–Strain Response and Springback Behavior," J. of Materi Eng and Perform, vol. 30, no. 1, S. 33–41, 2021.

[4] M. Firat, B. Kaftanoglu, and O. Eser, "Sheet metal forming analyses with an emphasis on the springback deformation," Journal of Materials Processing Technology, vol. 196, 1-3, S. 135–148, 2008.

[5] J. L. Chaboche and G. Rousselier, "On the Plastic and Viscoplastic Constitutive Equations—Part II: Application of Internal Variable Concepts to the 316 Stainless Steel," Journal of Pressure Vessel Technology, vol. 105, no. 2, S. 159–164, 1983.

[6] F. Yoshida and T. Uemori, "A model of large-strain cyclic plasticity describing the Bauschinger effect and workhardening stagnation," International Journal of Plasticity, 2001.

[7] D. Staud and M. Merklein, "Tagungsband_Werkstoffpruefung_2009.pdf," Tagungsband Werkstoffprüfung, S. 211–218, 2009.

[8] J. Kim, G. H. Gu, J. Kwon, M. H. Seo, and H. S. Kim, "A Novel Framework for Evaluating the Intrinsic Mechanical Properties of Sheet Metals Using Two-dimensional Digital Image Correlation," Met. Mater. Int., vol. 31, no. 10, S. 2837–2844, 2025.

[9] J. Bauschinger, Über die Veränderung der Elastizitätsgrenze und die Festigkeit des Eisens und Stahls durch Strecken und Quetschen, durch Erwärmen und Abkühlen und durch oftmals wiederholte Beanspruchungen: Königliche Technische Hochschule München, 1886.

[10] K. Watanabe, K. Natori, T. Tanaka, and Y. Imaida, "Study on the Bauschinger effect with increasing of tensile strength in dual phase steel sheets," in *High Performance Structures and Materials V*, Tallinn, Estonia, 2010, S. 119–131.

[11] O. Majidi, F. Barlat, M.-G. Lee, and D.-J. Kim, "Formability of AHSS under an Attach–Detach Forming Mode," steel research int., vol. 86, no. 2, S. 98–109, 2015.

[12] V. I. Dotsenko, "Stress Relaxation in Crystals," Physica Status Solidi (b), vol. 93, no. 1, S. 11–43, 1979.

[13] K. Hariharan, P. Dubey, and J. Jain, "Time dependent ductility improvement of stainless steel SS 316 using stress relaxation," Materials Science and Engineering: A, vol. 673, S. 250–256, 2016.

[14] D. Naumann and M. Merklein, "Influence of an optical strain rate controlled tensile testing method on mechanical properties of sheet metals," in *Material Forming: ESAFORM 2024*, 2024, S. 922–929.

[15] C. Suchocki and Z. Kowalewski, "A new method for identification of cyclic plasticity model parameters," Archiv.Civ.Mech.Eng, vol. 22, no. 2, 2022.

[16] A. H. Mahmoudi, S. M. Pezeshki-Najafabadi, and H. Badnava, "Parameter determination of Chaboche kinematic hardening model using a multi objective Genetic Algorithm," Computational Materials Science, vol. 50, no. 3, S. 1114–1122, 2011.

[17] M. Rosenschon and M. Merklein, "Analysis of the stress and directional dependent Bauschinger-effect of sheet metals," IDDRG 2018, 2018.